Transfer Matrix Based Semiclassical Model for Field-induced and Geometrical Quantum Confinement in Tunnel FETs

Saurabh Sant, Hamilton Carrillo-Nuñez, Mathieu Luisier, and Andreas Schenk
Integrated Systems Laboratory, ETH Zurich, CH-8092 Zurich, Switzerland.
Email: sasant@iis.ee.ethz.ch

***Abstract*— The paper presents a semi-classical model to take into account the effect of field induced as well as geometric quantization. It uses the transfer matrix method to determine whether the energy of a given tunnel path lies above or below the first sub-band level. The validity of the model is verified by simulating transfer characteristics of a one-dimensional InGaAs/GaAsSb n-channel TFET and comparing the result with those of quantum-mechanical calculations. Furthermore, the good agreement between transfer characteristics of InAs/Si bilayer TFETs obtained by 2D semi-classical simulations with those found by OMEN simulations suggests that the developed model is also useful for 2D devices. It also implies that, replacing a rigid 2D TFET simulation by semi-classical 1D simulations along straight tunnel paths is a viable TCAD approach.**

***Keywords*—Tunnel FET, Line Tunneling, Gemoetrical quantum confinement, field induced quatum confinement**

I. Introduction

Tunnel Field Effect transistors (TFETs) are considered as viable alternatives for MOSFETs in low-power electronic applications. In a TFET, band-to-band tunneling (BTBT) can take place normal to the gate (often called line tunneling) or can occur parallel to the gate between the source and the gate (often called point tunneling).

Line tunneling begins when the device is under strong inversion. Under such conditions, a triangular-like quantum well in the channel quantizes the electronic states. This delays the onset of line tunneling and reduces the strength of tunneling [1,2]. This effect can be included in a semi-classical framework using a model based on the "path rejection method"[1]. In this model, a tunnel path is accepted if its energy is above the first sub-band level, but is rejected otherwise. In this case, the sub-band energy arising from the bottom of the triangular-like well is calculated by the triangular well approximation. This model is not applicable in the presence of pocket counter-doping, as the approximation is no longer valid. In certain device geometries (see e.g. Fig. 2(a-1,2,3)), confinement arising from hetero-junctions adjacent to the gate is superimposed on the triangular-like well. This changes the energy level of the 1st sub-band. In this paper, we present a transfer matrix based model that accounts for the effects of quantization due to an arbitrary band-edge profile.

II. Description of the Model

Implementation of the quantization model for a one-dimensional device is schematically given in Fig. 1(a). Tunnel paths which begin at the valence band (VB) edge and end at the conduction band (CB) edge are determined from the band diagram. The tunnel paths are then extended till the oxide interface. The transfer matrix is evaluated along the line between the starting point of the tunnel path and the oxide/semiconductor interface. It is evaluated at three energy points, namely, the tunnel path energy, the energy of the CB edge at the oxide/semiconductor interface (i.e. bottom of the well), and at the middle of these energy points. If the transfer matrix element $t_{11}(E)$ changes its sign between consecutive energy points, it implies that the sub-band level lies below the tunnel path energy (see Fig. 1(b)). In that case, the tunnel path is accepted. It is rejected otherwise. The above model requires the evaluation of the transfer matrix element at three energy points. Therefore, the model is computationally slightly more expensive than the one which uses the triangular well approximation.

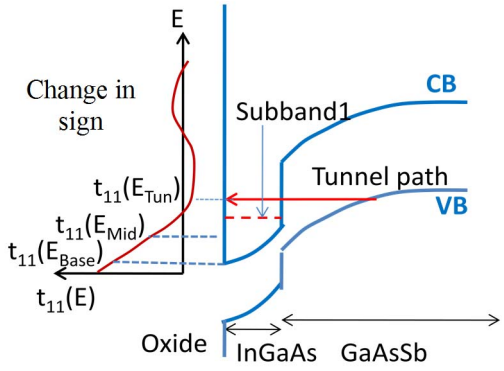

Figure 1: Schematic of the proposed semi-classical model to take into account the geometric confinement effect. The model is based on the path rejection technique and uses the transfer matrix method to check whether the tunnel path lies above the first sub-band level or not.

III. Application to (pseudo) 1D Device

The one-dimensional vertical cross section of an $In_{0.7}Ga_{0.3}As/GaAs_{0.36}Sb_{0.64}$ vertical TFET (Fig. 1(b)) was simulated using a 1D k·p-Poisson solver available in S-Band [4]. For each gate bias, the energy levels and the quantized wave functions of the first sub-band were extracted from the simulations. The Numerov method was used to obtain the VB wave functions in the bulk for all $E_\perp$ in the tunnel window. The transmission probability was calculated for each $E_\perp$ using Fermi's Golden Rule. The total vertical tunnel current was then evaluated using the Landauer formalism by integrating $E_\perp$ over the available tunnel window. This procedure is discussed in detail below.

Because of the confining potential well in the channel, the CB states are quantized. They were obtained by solving the following envelope equation numerically using a 1D k·p-Poisson solver available in S-Band [5]:

Funding from the European Community's Seventh Frame-work Program under Grant Agreement No. 619509 (Project E2SWITCH) is acknowledged.

978-1-5090-0818-6/16/$31.00 ©2016 IEEE

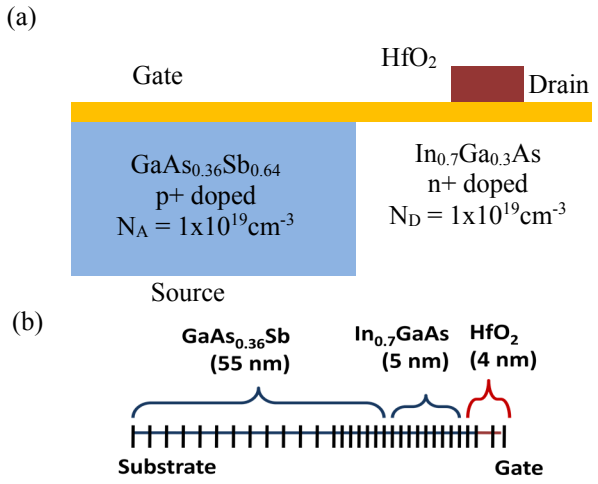

Figure 2: (a) InGaAs vertical TFET with counter-doped pocket. The special geometry favors line tunneling and is used to analyze the impact of channel quantization on line tunneling. (b) 1D cross-section of the above pseudo-one dimensional TFETs simulated using S-Band.

$$\left(-\frac{\hbar^2}{2m_c}\frac{d^2}{dx^2}+U(x)\right)\cdot\chi_{c,n}(x)=E_n\cdot\chi_{c,n}(x). \quad (1)$$

For Eq. (1) it has to be assumed that the device is invariant in the yz-plane. Hence, y- and z-dependent components of the envelope function are given by plane waves. This adds an additional energy term to the total energy. The total energy thus becomes $E_n^{\perp}=E_n+E^{\perp}$.

Since VB states are not quantized, an envelope function exists for each value of available $E^{\perp}$. The envelope functions for the VB states were obtained solving the following equation using the Numerov algorithm:

$$\left(-\frac{\hbar^2}{2m_v}\frac{d^2}{dx^2}+(U(x)-E-E')\right)\cdot\chi_v(x,E')=0. \quad (1)$$

Hard-wall boundary conditions at the oxide-semiconductor interface $(\chi_v(x=0,E^{\perp})=0)$ were used as boundary condition for the wave function as required for the Numerov algorithm.

The envelope functions for the CB and VB states obtained by the above method are exact solutions of the Schrödinger envelope equation. The inter-band matrix element as a function of $E^{\perp}$ can be obtained by treating the field-dependent inter-band coupling term as perturbation,

$$M_{n,v}(E_n^{\perp},E')=\int_0^{\infty}\chi_{c,n}(x)\cdot H'(x)\cdot\chi_v(x,E')dx, \quad (2)$$

$$\text{where } H'(x)=\frac{\hbar\cdot P}{m_0\cdot E_g}\nabla\mathrm{U(x)}.$$

Here, P is the momentum matrix element and E_g is the band gap. The tunnel probability can then be calculated using Fermi's golden rule,

$$T(E')=\frac{2\pi}{\hbar}\int_{E_n}^{E_n+E_{max}}\left|M_{n,v}(E_n^{\perp},E')\right|^2\delta(E_n^{\perp}-E')dE_n^{\perp}. \quad (3)$$

Note that although E_n is discrete, $E_n^{\perp}$ is continuous as it involves the transverse energies. The above integral gives a Heaviside function on integration, which implies that $E'>E_n$ for tunneling to take place. The total electron current can be calculated by integrating the tunnel probability over all available transverse energies,

$$J_T=\int_0^{Emax}T(E'^{\perp})\rho(E'^{\perp})dE'^{\perp}. \quad (4)$$

The current density obtained by this approach is in the units A/m^2. It can be multiplied by the gate area to obtain the drain current.

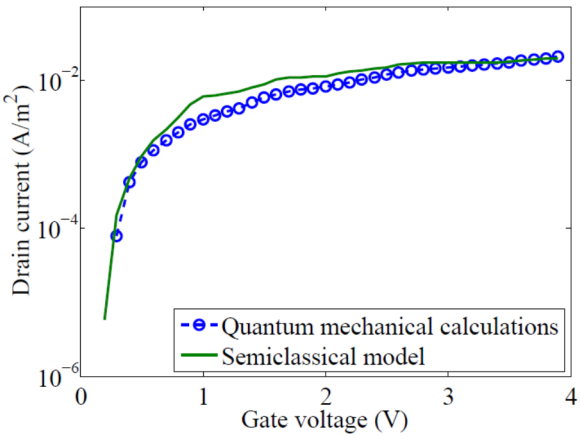

Figure 3: Comparison of the drain current of the one-dimensional TFET in Fig. 2(b) obtained by quantum-mechanical calculations with the current calculated using the semi-classical model.

The transfer matrix based channel quantization model was used to semi-classically compute the tunnel current with the band edge profiles obtained from S-Band. The model described in Section II was employed to obtain the generation rate at each discretization point in the one-dimensional device. This generation rate was integrated over z to obtain the drain current density as described below:

In the modified dynamic nonlocal path BTBT model implemented in S-Device [3], the generation rate of electrons and holes is given by

$$G_{cv}(x,E_t)=\nabla U(x)\frac{g}{18\hbar}\exp\left(-2\int_0^L\kappa(l)dl\right)\cdot\frac{1-\exp\left(-k_m^2\int_0^L\kappa(l)^{-1}dl\right)}{\int_0^L\kappa(l)^{-1}dl}\cdot\left[f\left(\frac{E_t-F_n(L)}{kT}\right)-f\left(\frac{E_t-F_p(0)}{kT}\right)\right]\cdot\Theta(E_t-E_0) \quad (5)$$

where E is the energy of the tunnel path, x the position of the discretization point, l the distance along the tunnel path, $\int_0^l\kappa(x)dx$ the action integral over the imaginary dispersion along the tunnel path, $\hbar k_m^2/2m_e$ the maximum transverse energy of a tunneling electron, $f(x)$ the Fermi distribution function, $\Theta(x)$ denotes the Heaviside function, and E_0 is energy of the first sub-band. The additional factor $\Theta(x)$ in the above equation implies that the generation rate is calculated only if the tunnel path lies above the first sub-band energy. This $\Theta(x)$ factor is equivalent to the transfer matrix based path rejection method described in Section II. The generation rate (5) at each vertex is summed over the entire device area to calculate the tunnel current. Only the tunnel paths with energy above the first sub-band level are selected in the integration.

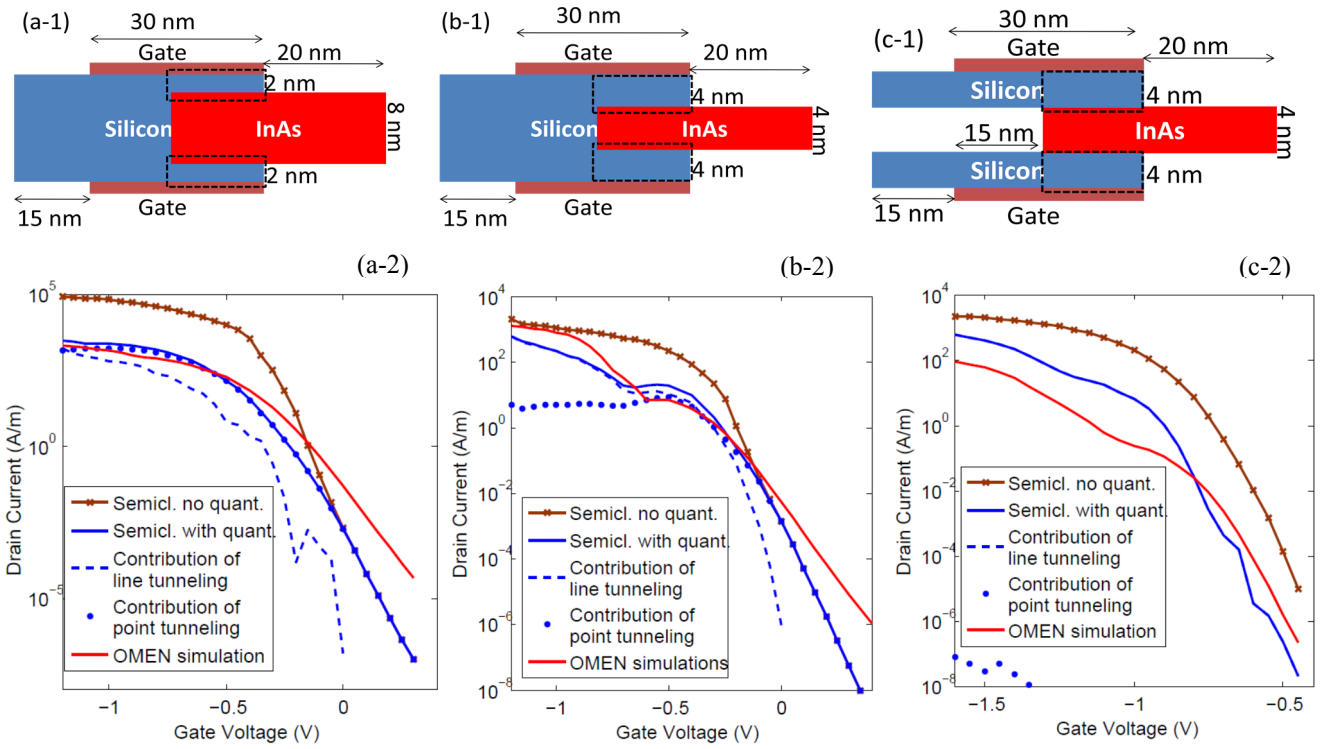

Figure 4: (a-1, b-1, c-1) 2D device geometries of InAs/Si bilayer TFETs simulated with both the full-band quantum transport solver OMEN and the semi-classical model in S-Device. The box in each figure shows the region where the channel quantization model was activated. (a-2, b-2, c-2) Comparison of transfer characteristics simulated by OMEN with the ones simulated using the transfer matrix based semi-classical model.

Therefore,

$$J_D(V_{GS}) = \int_0^T G_{cv}(x, E_V(x))dx \qquad (6)$$

where T is the thickness of the device,E_0 is the energy of the first sub-band. In the dynamic non-local path model, the energy of a tunnel path is set to the energy of the VB edge at the starting point($E_t = E_V(x)$). In a 1D device like the one in Fig. 2(b), the transfer matrix based model presented in Section II is equivalent to multiplying the tunnel rate with the Heaviside function.

The comparison of semi-classical treatment and one-band envelope method is presented in Fig. 3. The very good agreement between the two approaches verifies the validity of the semi-classical model for a (pseudo-)one-dimensional device.

IV. Implementation for 2D device simulations

In order to implement the above semi-classical model for 2D device simulations, one needs to convert the 2D simulation problem to a number of 1Dproblems. This is achieved by extracting the tunnel paths from the 2D band edge diagram of the TFET. Each tunnel path starts from the CB edge, continues in the direction of the electric field, and ends at the VB edge. This tunnel path is then extended by up to 8nm beyond its end point. If the extension intersects the oxide/semiconductor interface, the tunnel path is counted as a "line tunnel path". Otherwise it is considered as a "point tunnel path". The tunnel path is also extended by up to 8nm before its starting point. The channel quantization model is not applied on point tunnel paths as tunneling is not affected by channel quantization here. On line tunnel paths it is applied as follows: If the extension of the tunnel path intersects the oxide/semiconductor interface, the band diagram and effective masses along the tunnel path are extracted. These quantities are then used to evaluate the transfer matrix at three energy values as explained earlier. Based on whether $t_{11}(E)$ changes its sign, the tunnel path is either selected or rejected. If the tunnel path is selected, the tunnel current is evaluated using Kane's WKB theory of BTBT which involves integration over the imaginary E-k relation [6]. For the latter, Flietner's two-band model [7] was used.

In order to reduce the computational burden, the channel quantization model based on the path rejection method is applied only in those regions where the tunnel paths are likely to intersect the oxide-semiconductor interface. The dimensions of these regions have to be specified by the user.

V. Simulation results and Discussion

The above-described implementation of the transfer matrix based channel quantization model was employed for the semi-classical simulation of InAs/Si bilayer TFETs in Figs. 4(a-1), 4(b-1), and 4(c-1).The same TFETs had been simulated using the full-band quantum transport simulator OMEN in an earlier work [5]. There, electrostatic potential, effective masses and the band gap were obtained from OMEN simulations at each bias point [5]. The same electrostatic potential was used here to extract semi-classical tunnel paths in the above devices. The transfer matrix based channel quantization model was applied on these paths to calculate the BTBT rate. The generation rate in the whole device area was then integrated to obtain the total drain current:

$$I_D\,(V_{GS}) = \int_0^T \int_0^W G_{cv}(x, y, E_V(x, y))dxdy \qquad (7)$$

Here, I_D is the drain current per unit width of the device. In a 2D device, the transfer matrix based model is applied independently along each tunnel direction resulting in

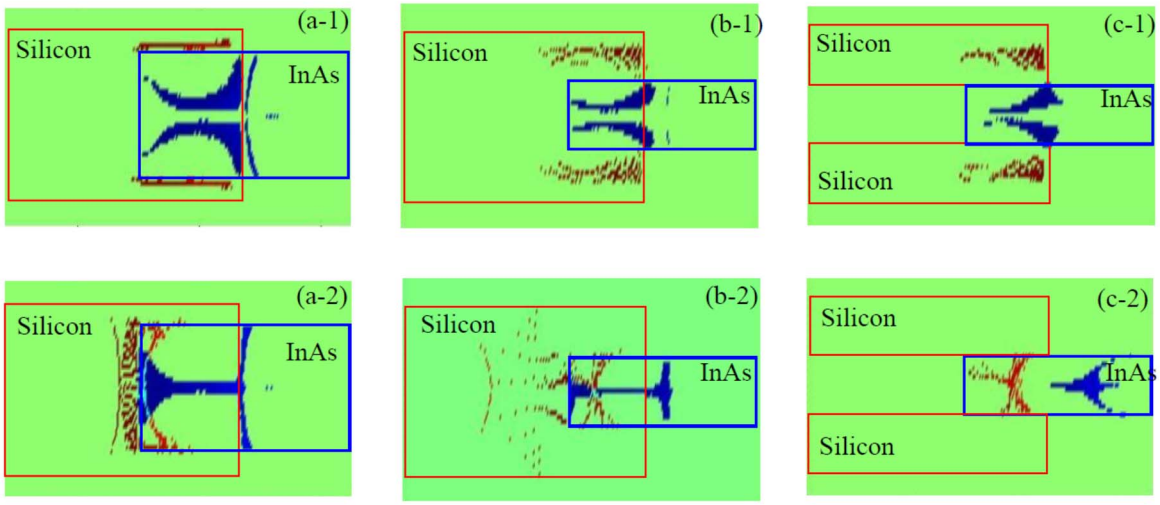

Figure 5: (a-1, b-1, c-1) Color-mapped diagrams showing the regions of electron generation (blue) and hole generation (red) in the ON-state by line tunneling. Channel quantization model has been included in the simulation. (a-2, b-2, c-2) Color-mapped diagram showing electron and hole generation by point tunneling in the ON-state.

different sub-band energy levels for different tunnel paths. If a tunnel path lies energetically below the first sub-band level, it does not contribute to the generation rate. The above procedure implicitly assumes ballistic transport of the carriers in the device. The same approximation had been used in the full-band OMEN simulations.

Transfer characteristics obtained from OMEN and the semi-classical simulation are presented in Figs. 4(a-2), 4(b-2), and 4(c-2). Contributions from line and point tunneling have been separated in the semi-classical simulations and are also shown along with the total drain current. The semi-classical simulations show good agreement with the OMEN results suggesting that the proposed model is able to take into account the effect of channel quantization and geometric confinement quantization within a semi-classical framework. The comparison of individual contributions of line and point tunneling implies that point tunneling is the major contributor in TFET-A, although the contribution of line tunneling cannot be ignored. In TFET-B, point tunneling is the major contributor to the drain current in the subthreshold region while line tunneling begins to dominate at $V_{GS} \sim 0.7$ eV resulting in a kink in the transfer characteristics. Such a kink is also observed in the OMEN results at nearly the same gate bias. In TFET-C, tunneling is exclusively line tunneling, due to geometric restrictions on the tunnel direction.

Color-mapped diagrams of BTBT generation rate in the devices in ON-state have been plotted in Figs. 5(a-1), 5(b-1), and 5(c-1) for line tunneling and Figs. 5(a-2), 5(b-2), and 5(c-2) for point tunneling. In all the three TFETs, hole generation by line tunneling is shifted away from the oxide-Silicon interface. This is a consequence of field-induced and geometrical quantization.

Semi-classical transfer characteristics and the ones obtained by full-band simulation do not match well in the sub-threshold region as observed in Fig. 4(a-2) and Fig. 4(b-2). In this region, the transfer characteristics are dominated by point tunneling for which the proposed semi-classical model is not applicable. A possible explanation for the discrepancy could be that only the Γ-point was used in the OMEN simulations of TFET-A and TFET-B to save CPU time. This simplification results in an over-estimation of the drain current in the sub-threshold regime of these devices. In the OMEN simulation of TFET-C, a multiple k-point grid was used giving a smaller SS which better agrees with the semi-classical curve. Furthermore, the self-consistent electrostatics from OMEN was used in the semi-classical model. Using the electrostatics from S-Device (Poisson and drift-diffusion equations) instead would lead to some small differences.

VI. Conclusion

A semi-classical model to take into account the effect of field-induced as well as geometrical quantization is proposed. The model uses the transfer matrix method to determine whether the energy of a given tunnel path lies above or below the first sub-band level. The validity of the model was verified by simulating transfer characteristics of a one-dimensional InGaAs/GaAsSb n-channel TFET and comparing the result with those of quantum-mechanical calculations. Furthermore, the good agreement between transfer characteristics of InAs/Si bilayer TFETs obtained by 2D semi-classical simulations with those found by OMEN simulations suggests that the developed model is also useful for 2D devices. It has been shown that replacing a rigid 2D TFET simulation by semi-classical 1D simulations along straight tunnel paths is a viable TCAD approach.

References:

[1] W. Vandenberghe, B. Sorée, W. Magnus, G. Groeseneken, A. Verhulst and M. Fischetti, “Field Induced Quantum Confinement in Indirect Semiconductors: Quantum Mechanical and a Modified Semiclassical Model”, SISPAD 2011, p. 271, 2011.

[2] A. Schenk, S. Sant, K. Moselund, and H. Riel, “III-V-Based Hetero Tunnel FETs: A Simulation Study Focussed on Non-ideality Effects“,Proc. ULIS-EUROSOI, pp. 9-12, Wien 2016.

[3] Synopsys Inc., Sentaurus Device User Guide, V- 2015.06.

[4] Synopsys Inc., Device MonteCarloUser Guide, V-2015.06.

[5] H. Carrillo-Nuñez, M. Luiser, and A. Schenk, “Analysis of InAs-Si Heterojunction Double-Gate Tunnel FETs with Vertical Tunnel Paths”, Proc. ESSDERC pp. 302-305, 2015.

[6] E. O. Kane, “Zener Tunneling in Semiconductors”, J. Phys. Chem. Solids vol. 12, pp. 181-181, 1959.

[7] H. Flietner, “The E(k) relation for a 2-band scheme of semiconductors and the application to metal-semiconductor contact,” Phys. Stat. Sol. (b), vol. 54, pp. 201-208, 1972.